Journal of Applied Electrochemistry **32**: 1141–1149, 2002.

Electrodeposition and properties of cyclically modulated silver–antimony alloys

I. KRASTEV[1,*] and A. ZIELONKA[2]
[1]*Institute of Physical Chemistry, Bulgarian Academy of Sciences, 1113 Sofia, Bulgaria*
[2]*Forschungsinstitut für Edelmetalle und Metallchemie, 73525 Schwäbisch Gmünd, Germany*
*(*author for correspondence)*

Received 23 October 2001; accepted in revised form 20 June 2002

Key words: coating properties, cyclically modulated alloys, electrodeposition, internal stress, silver–antimony alloys

Abstract

An investigation was carried out on the influence of electrodeposition conditions on the properties of cyclically modulated Ag–Sb alloys, such as internal stress, microhardness, roughness, electrical contact resistance, wear resistance and plug-in forces. Pulses of different amplitude and duration were used, leading to different composition and thickness of the deposited sublayers, and the resulting changes in the coating properties were demonstrated. The possibility of depositing coatings free of internal stress is shown. The electrical contact resistance does not depend on the multilayer structure of the coating, but on the type and properties of the upper sublayer. The microhardness of the multilayer coatings increases with the increase in their antimony content. It decreases for very short pulses whereby the effect of the higher current density cannot be realized. The wear resistance of the multilayer coatings displays values between those of the respective monolayer coatings deposited under the conditions of separate sublayer deposition. It increases at a very small sublayer thickness, at decreasing contribution of the higher current density and at lower stress values of the multilayer coatings. The roughness of the coatings is not influenced by their multilayer structure, and the plug-in forces increase with the reduction of the sublayer thickness to about 0.03 μm.

1. Introduction

Interest in the electrolytic deposition of silver–antimony alloys is based on the possibility of depositing layers of improved mechanical and tribological properties compared to pure silver coatings [1–3], and of studying the self-organization phenomena under electrochemically well controlled conditions [4].

A series of previous papers presents investigations on the electrodeposition of silver [5], on the phase and elemental composition of the deposited alloy [6], on the structure of the electrodeposits [7–9], on the cathodic current oscillations with time under potentiostatic conditions [10, 11], on the influence of convection [12], as well as on the electrical [13] and mechanical properties of the deposited alloys [14]. The propagation of waves of different phases on the electrode surface during deposition results in the spontaneous development of multilayer systems of interesting and unexpected properties [11, 13]. The phases of the silver–antimony alloy differ in colour, thus allowing the visualization of the developing surface structures and the deposited multilayer structures, respectively.

Multilayer structures can be obtained by applying appropriate current pulses or by modification of the electrolysis conditions. These multilayer structures are expected to show better properties of the coatings than the separate metals.

This paper describes the electrodeposition of cyclically modulated silver–antimony alloys; their properties are compared to those of the respective thick alloy layers.

2. Experimental details

The investigations were carried out with a ferrocyanide–thiocyanate electrolyte for silver–antimony deposition [2, 4, 6–14]. The method of preparation and the electrochemical properties of this electrolyte were described recently [5]. The silver cyanide complex was formed by boiling together $AgNO_3$, $K_4Fe(CN)_6$ and K_2CO_3 for several hours. After cooling and removal of the iron hydroxide precipitate, the solution was analysed and used in different concentrations for the preparation of the electrolyte. The electrolyte composition is given in Table 1.

Measurements were carried out on internal stress, IS (FEM, Stalzer [18]), electrical contact resistance, R_Ω (Burster, Resistomat 2323), Vickers microhardness, *Hv* (Leitz, Durimet II and Reichert–Jung, Micro-Duromat 4000E Polyvar), wear resistance, *A* (Boch–Weinmann test, Erichsen, Modell 317), roughness, *Ra* (Perthen, Perthometer), and the plug-in forces, *F* (FEM, Steckkraftmessgerät). The methods of measurement of the deposit properties were described in detail in a previous paper [14].

Table 1. Electrolyte composition

Component	Concentration/g dm^{-3}
Ag	16
$K_4Fe(CN)_6 \cdot 3H_2O$	70–90
K_2CO_3	20
KSCN	150
$KNaC_4H_4O_6 \cdot 4H_2O$	60
Sb as $K(SbO)C_4H_4O_6 \cdot 1/2H_2O$	5.0–7.5

The alloy electrodeposition was performed galvanostatically on copper substrates by means of a pulse generator (Pragmatic Instruments, Pragmatic 2411A) and a bipolar operational amplifier (Kepco, BOP 20-10 M). In most cases, the current parameter were chosen so as to ensure the development of equally thick sublayers of the respective alloys. By decreasing the thickness of these sublayers, coatings of different overall composition were obtained and their properties were investigated. The internal stress was monitored *in situ* during deposition and the rest of the layer parameters with the exception of electrical contact resistance and plug-in forces, were measured after deposition on the same samples, thus allowing direct comparison of the results of all measurements.

3. Results

3.1. *Internal stress*

By variation of the electrolysis conditions, internal stress of different values and signs could be developed in the alloy layers [14]. It was shown that at metal ion concentrations $C_{Ag} = 16$ g dm^{-3} and $C_{Sb} = 7.5$ g dm^{-3} and current density, J, of 0.5 A dm^{-2}, layers of negative (compressive) internal stress, are deposited, which is due to codeposition of antimony and to extension of the silver lattice.

At a higher current density ($J = 0.75$ A dm^{-2}), the silver lattice is saturated with antimony, a new antimony-richer phase is deposited, and the compressive stress decreases. With further increase of J (1 A dm^{-2}), the compressive stress changes into tensile stress [14]. Under such conditions, one can observe the formation and propagation of dynamic space–time structures on the electrode surface [4, 7–12, 14]. They consist of phases with different Sb-content and can be observed as waves, targets and spirals with different numbers of arms. The origin is an electrochemical instability induced by natural convection in the electrolyte [12].

The parameters of the current pulses for the cyclically modulated alloys were chosen in such a way that the respective sublayers corresponded to the above two cases [15]. Internal stress (IS) measurements in cyclically modulated layers using different methods are described in [16, 17]. Using the apparatus constructed by Stalzer [18], which operates on the principle of the one-sidedly galvanized bendable cathode, the IS changes can be monitored *in situ* during the deposition of the multilayer coatings. The results of the stress measurements are presented as the output voltage of the sensor, which is more informative than the calculated IS values [14].

Figure 1 shows the electric signal detected by the sensor for the two thick alloy layers and for the multilayer coating, respectively. Under identical conditions, IS is proportional to the slope of the respective curve. The internal stress of the first sublayers corre-

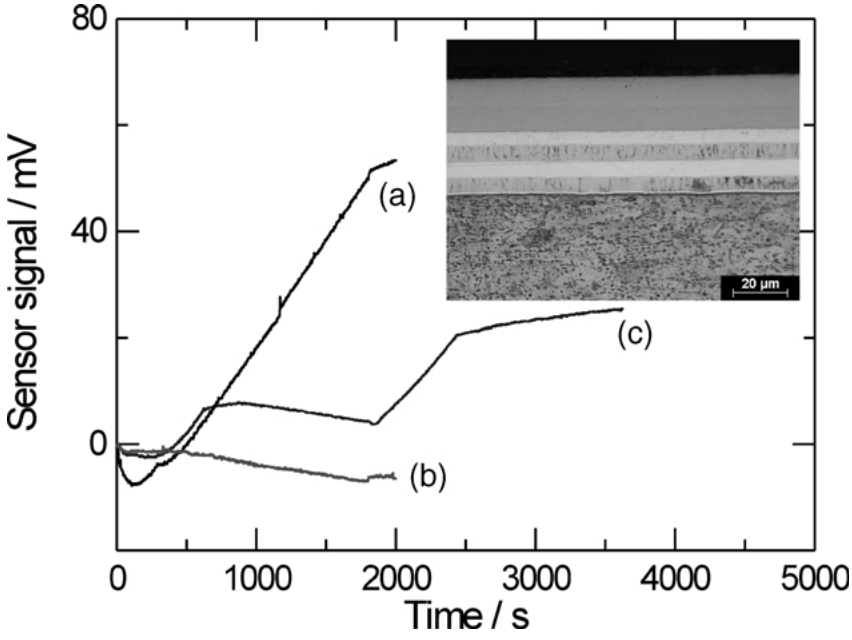

Fig. 1. Time dependence of the sensor signal during IS measurement of thick alloy layers and multilayer coatings. $C_{Ag} = 16$ g dm^{-3}; $C_{Sb} = 7.5$ g dm^{-3}. Curves: (a) 1 A dm^{-2}, IS = +2.86 kp mm^{-2}; (b) 0.5 A dm^{-2}, IS = −0.57 kp mm^{-2}; (c) 10 min, 1 A dm^{-2} and 20 min, 0.5 A dm^{-2}. Inset: cross-section of the multilayer coating (1 kp= 9,80665 N).

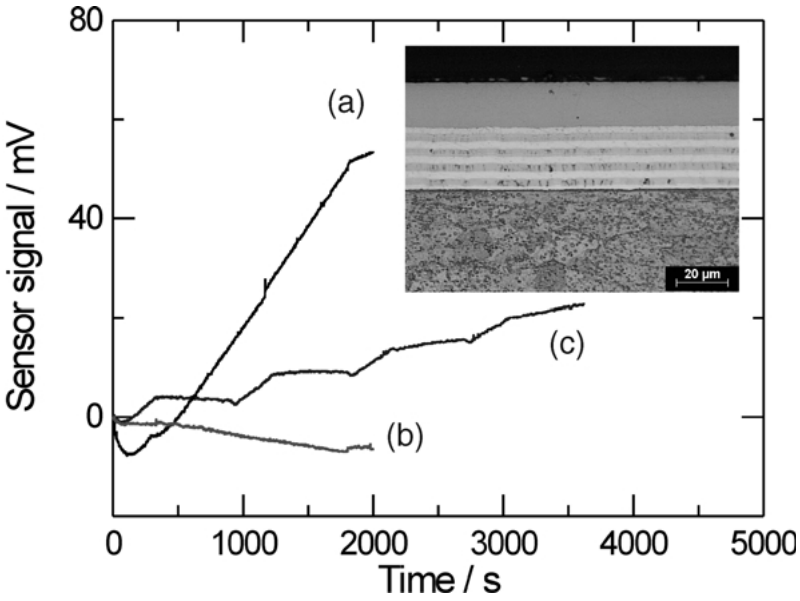

Fig. 2. Time dependence of the sensor signal during IS measurement of thick alloy layers and multilayer coatings. $C_{Ag} = 16$ g dm^{-3}; $C_{Sb} = 7.5$ g dm^{-3}. Curves: (a) 1 A dm^{-2}; (b) 0.5 A dm^{-2}; (c) 5 min, 1 A dm^{-2} and 10 min, 0.5 A dm^{-2}. Inset: cross-section of the multilayer coating.

sponds to the stress of a thick alloy coating of the same composition. The stress in the next sublayers is influenced by the previous sublayers and a change is observed in the slope of the respective parts of the curves.

The cross section of the same multilayer sample is shown as an inset in Figure 1. Despite the high current density in the initial stage, deposition of the more precious silver prevails until its concentration at the surface of the cathode decreases to zero and the process becomes diffusion-controlled. Only then does the antimony deposition become noticeable. During this initial period, changes are also observed in the trend of the sensor signal curve, which takes its stationary shape (corresponding to the bulk deposit) only after the transition of the internal stress from compressive to tensile.

Figures 2 and 3 show the IS curves for shorter electrodeposition periods and their gradual approach to a straight line. The respective cross sections (insets in

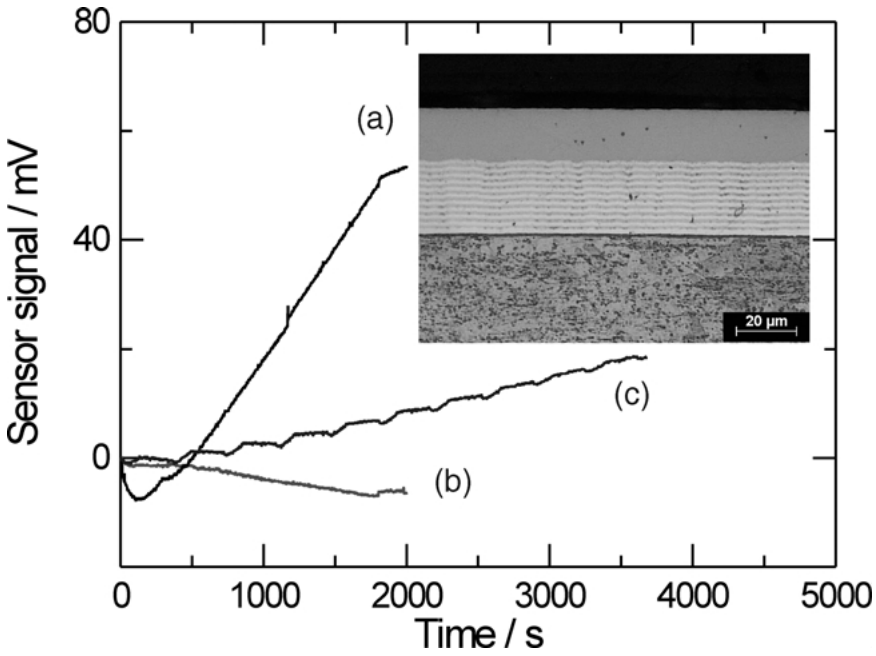

Fig. 3. Time dependence of the sensor signal during IS measurement of thick alloy layers and multilayer coatings. $C_{Ag} = 16$ g dm^{-3}; $C_{Sb} = 7.5$ g dm^{-3}. Curves: (a) 1 A dm^{-2}; (b) 0.5 A dm^{-2}; (c) 1 min, 1 A dm^{-2} and 2 min, 0.5 A dm^{-2}. Inset: cross-section of the multilayer coating.

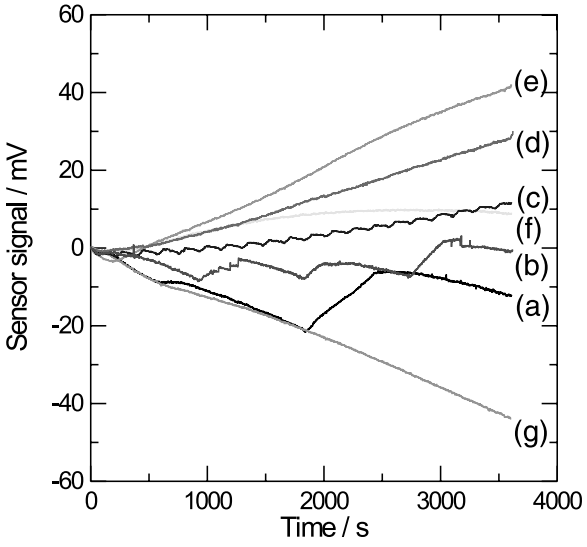

Fig. 4. IS changes depending on the pulse duration. $C_{Ag} = 16$ g dm^{-3}; $C_{Sb} = 7.5$ g dm^{-3}. Current density ratio 1 A dm^{-2}/0.5 A dm^{-2}. Pulse durations: (a) 10 min/20 min, (b) 5 min/10 min, (c) 1 min/2 min, (d) 6 s/12 s, (e) 1 s/2 s, (f) 250 ms/500 ms and (g) 100 ms/200 ms.

Figures 2 and 3) demonstrate that the multilayer system becomes finer. The IS values of the multilayer system are situated between the stress values of the separate alloys and the influence of the higher current density is responsible for the positive (tensile) IS in this case.

Similarly to the sublayers presented in Figures 1–3, the sublayers of the multilayer systems in Figure 4(a)–(c) are of thickness in the macroscopic range. With further decrease of the cyclic modulation period, changes in IS are detected, which reflect the increased influence of the higher current density, that is, of the tensile stress resulting from the latter (Figure 4(d)–(e)). This means that, under the chosen deposition conditions, the compressive stress in the sublayers deposited at a low current density cannot compensate the tensile stress in the sublayers deposited at high current density.

At periods shorter than 1 s (Figure 4(f), (g)) the system fails to follow the pulse shape and the predominant tensile stress decreases. The short high current density pulse seems to be insufficient to ensure the deposition of the antimony-rich phase and deposition takes place at an intermediate current density, which is closer to the low current density.

Similar results are also observed under other electrolysis conditions. Figure 5 shows the behaviour of another electrolyte ($C_{Ag} = 16$ g dm^{-3}, $C_{Sb} = 5$ g dm^{-3}), prepared by using the complex silver salt $KAg(CN)_2$ [14], whereby the deposition is realized at $J =$ 0.25/1 A dm^{-2}. In this case, due to the lower C_{Sb}, the thick alloy coatings deposited at a high current density exhibit compressive stress [14]. Again, the results show that the internal stress of the thick sublayers correspond to that of the thick alloy coatings (Figure 5(a)–(c)). By reducing the electrodeposition period, the increasing influence of the compressive stress is noticed (due to the high current density) (Figure 5(d)–(g)) and at very short

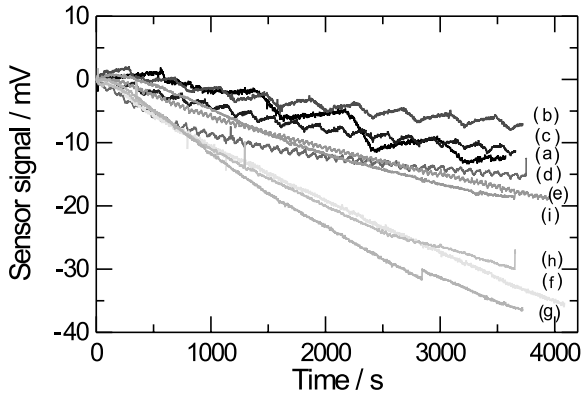

Fig. 5. IS changes depending on the pulse duration. $C_{Ag} = 16$ g dm^{-3}; $C_{Sb} = 5.0$ g dm^{-3}. Current density ratio 0.25 A dm^{-2}/1 A dm^{-2}. Pulse durations: (a) 550 s/250 s, (b) 275 s/125 s, (c) 138.5 s/62.5 s, (d) 55 s/25 s, (e) 27.5 s/12.5 s, (f) 13.85 s/6.25 s, (g) 5.5 s/2.5 s, (h) 2.75 s/1.25 s and (i) 1.138 s/0.625 s.

periods, corresponding theoretically to sublayer thickness in the nanometric range, a stress decrease is again detected, as if the high current density cannot produce its effect (Figure 5(h), (i)).

It is known that during pulse deposition higher J can be applied for a shorter time. Figure 6 shows a case of application of the high current density of 2 A dm^{-2}, the low current density being 0.25 A dm^{-2}. The duration of the pulses is chosen so that to ensure the pure silver sublayer deposited at low current density to be theoretically ten times thicker than the antimony-rich sublayer. For curve (a) (Figure 6), this would correspond to a sublayer thickness ratio of 2 μm to 0.2 μm, and for curve (d) – to a ratio of 0.1 to 0.01 μm. The antimony codeposited at the high current density induces a high tensile stress in the layer, as compared to the very low tensile stress upon deposition of pure silver layers at low current density. With increase in sublayer number this effect initially increases due to the rising number of the interfaces (curve (b)). At very short pulses the high current density is not effective and the tensile stress decreases (curves (c) and (d)).

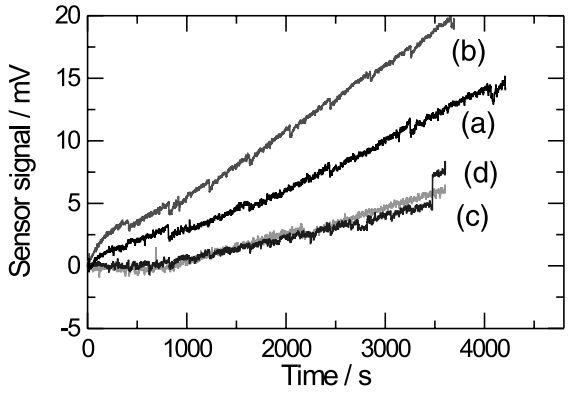

Fig. 6. IS changes depending on the pulse duration. $C_{Ag} = 16$ g dm^{-3}; $C_{Sb} = 7.5$ g dm^{-3}. Current density ratio 0.25 A dm^{-2}/2.0 A dm^{-2}. Pulse durations: (a) 800 s/12 s, (b) 400 s/6 s, (c) 200 s/3 s and (d) 40 s/0.6 s.

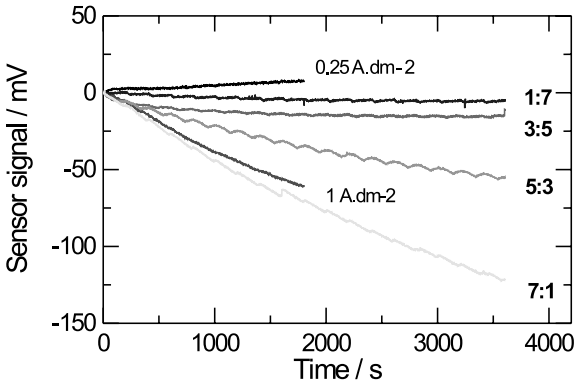

Fig. 7. IS changes depending on the pulse duration ratio: $C_{Ag} = 16$ g dm^{-3}; $C_{Sb} = 5.0$ g dm^{-3}. Ratio of the current densities 1.0 A dm^{-2}/0.25 A dm^{-2}. Frequency 5 mHz. Sum of both pulse durations = 200 s. 18 sublayer pairs. Pulse durations: (**1:7**) 25 s, 1.0 A dm^{-2}/175 s, 0.25 A dm^{-2}; 613 nm/sublayer pair; 11.04 μm. (**3:5**) 75 s, 1.0 A dm^{-2}/125 s, 0.25 A dm^{-2}; 927 nm/sublayer pair; 16.65 μm. (**5:3**) 125 s, 1.0 A dm^{-2}/75 s, 0.25 A dm^{-2}; 1195 nm/sublayer pair; 21.5 μm. (**7:1**) 175 s, 1.0 A dm^{-2}/25 s, 0.25 A dm^{-2}; 1508 nm/sublayer pair; 27.15 μm.

Figure 7 shows the influence of the thickness ratio of the two types of sublayers on IS. The total period of the two current pulses is 200 s and it is repeated 18 times in the course of the experiment. Eighteen pairs of sublayers of different thickness for different time ratios are deposited. Increasing the ratio of the two pulse durations, that is, the thickness of the sublayers in favour of the antimony-richer sublayer, the influence of the latter increases and the internal stress corresponds to the compressive stress of the thick alloy monolayer coatings deposited at high current density [14]. This conclusion is additionally confirmed by the cross-sections of the coatings (Figure 8(a)–(d)). Since the deposition time in these experiments is 1 h, the increase in the time ratio of high to low current density leads to multilayer coatings of greater total thickness.

Similar changes are observed when the deposition time for a sublayer pair is decreased to 20 and 2 s. A larger number of sublayer pairs (180 or 1800, respectively) were deposited for the same total deposition time. The dependence of the internal stress on the higher current density, that is, on the higher antimony content in the alloy is similar. The influence of the higher current density is not so clearly expressed when the deposition time for a sublayer pair is 2 s, it seems to be hampered by the very short pulse duration. The separate sublayers deposited at pulse periods of 2 and 20 s are sufficiently thin and cannot be observed in the optical microscope.

The results show that the high current density influences significantly the internal stress of the sublayer of high and intermediate thickness when the pulse duration ratio of the high current density to the lower

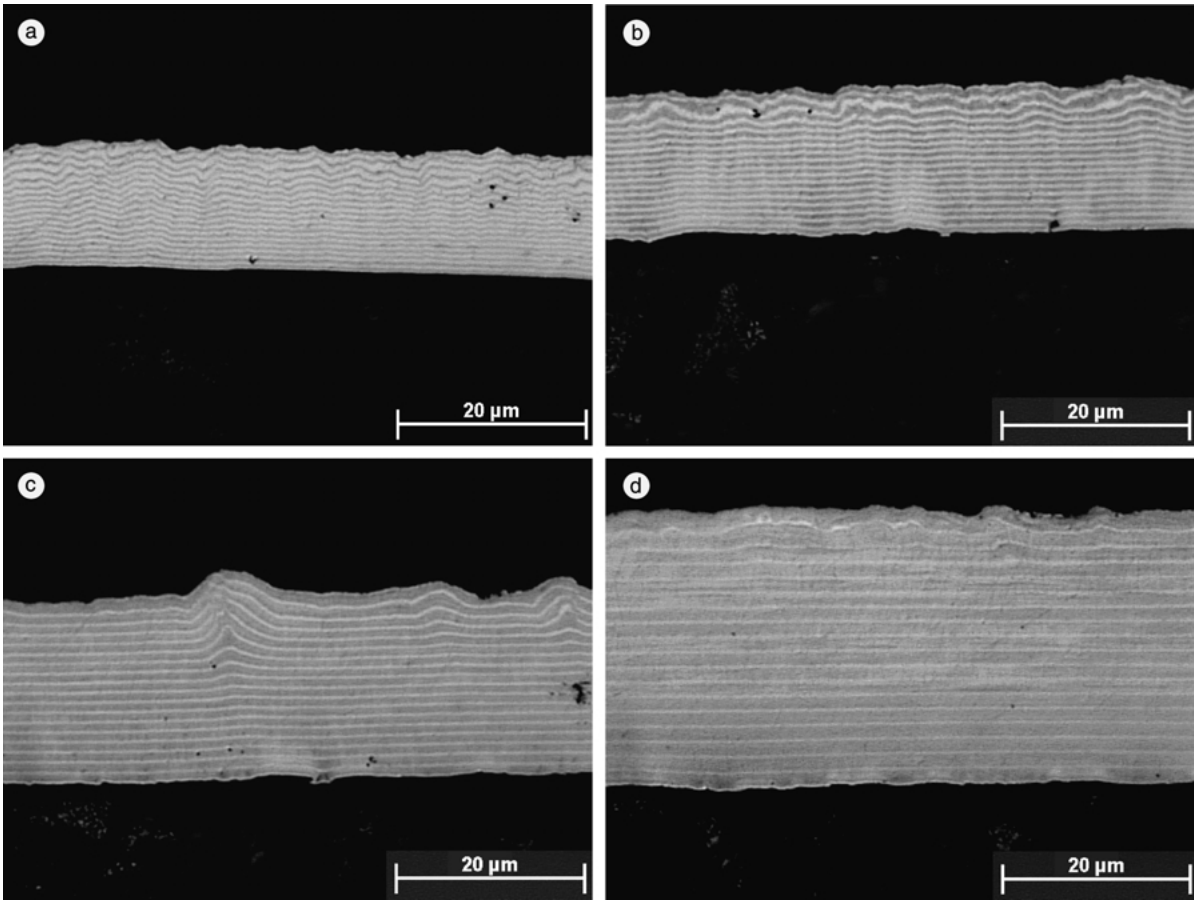

Fig. 8. Cross-sections of the multilayer coatings from Figure 7. Ratio of the pulse durations: (a) 1:7, (b) 3:5, (c) 5:3 and (d) 7:1.

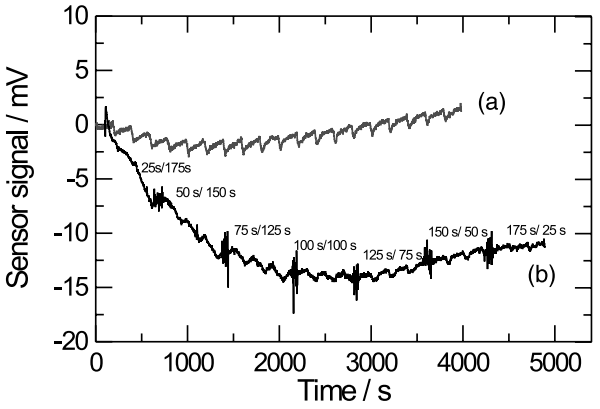

Fig. 9. IS changes depending on the pulse ratio (t_1:t_2) at a total period ($t_1 + t_2$) of 200 s. $C_{Ag} = 16$ g dm^{-3}; $C_{Sb} = 5.0$ g dm^{-3}; $KAg(CN)_2$ electrolyte. Ratio of the current densities 1.0 A dm^{-2}/0.25 A dm^{-2}. Key: (a) frequency 5 mHz; 175 s, 0.25 A dm^{-2}/25 s, 1.0 A dm^{-2}; (b) frequency 5 mHz; 25 s ÷ 175 s, 0.25 A dm^{-2}/175 s ÷ 25 s, 1.0 A dm^{-2}.

one is 7:1. At shorter pulses, the high current density is not effective and the compressive stress is reduced. In the other limiting case of pulse duration ratio of 1:7, the influence of the higher current density is not well expressed and the stress of the coating is independent of the sublayer thickness; practically unstrained coatings are obtained.

At a similar current density ratio, the thickness ratio of the separate sublayers is responsible for the IS value in the multilayer coating (Figure 9). By an appropriate choice of the pulse duration ratio, IS can be modified in such a way as to obtain layers of positive or negative stress, and even completely unstrained coatings. The time ratios presented in the figure correspond to the lower part of the total curve. However, it should be taken into account that the sublayer stress is influenced by the stress in the previous layers of the coating, so that the curve slope for the thick multilayer systems may slightly differ from the slope of the respective parts of the curve in Figure 9.

The IS measurements lead to the conclusion that the internal stress of the multilayer coating of the silver–antimony alloy can be modified conveniently by an appropriate variation of the pulse parameters.

3.2. *Electrical contact resistance*

The contact resistance, R_Ω, of 6 μm thick multilayers was measured by the Burster microohmmeter Resistomat 2323 on brass contact pins of diameter 4 mm and length 14 mm at a force of 2 N. R_Ω strongly depends on the type of the highest sublayer in the system. The separate sublayers were of equal thickness and were deposited at current densities of 1 and 0.5 A dm^{-2}, respectively.

Figure 10 shows the results obtained for R_Ω from measurements against gold-plated samples. The first point on the curve corresponds to multilayer systems of sublayer thickness of about 1 μm and the last point to

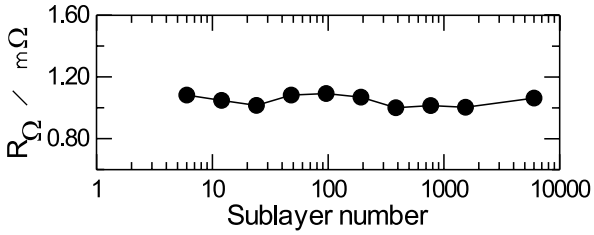

Fig. 10. Contact resistance of the 6 μm thick multilayer coatings depending on the number of sublayers. $C_{Ag} = 16$ g dm^{-3}; $C_{Sb} = 7.5$ g dm^{-3}. Ratio of the current densities J_1:$J_2 = 1$ A dm^{-2}/0.5 A dm^{-2}. Ratio of pulse durations: t_1:$t_2 = 1$:2.

the theoretical thickness of 1 nm. The measurement on coatings with a thicker sublayer was irrelevant. In this case, R_Ω of the respective alloy phases would be measured, as described elsewhere [14]. The results show that R_Ω is of approximately constant value and is independent of the number, that is, of the thickness of the deposited sublayers. The deviations are due to changes in the surface layer. The value of R_Ω corresponds to an alloy composition which, in the case of the thick monolayer coatings, is deposited from the same electrolyte at a current density of about 0.75–0.8 A dm^{-2} [14].

3.3. *Microhardness*

The alloying of silver with antimony aims at the enhancement of the hardness and wear resistance [1–3]. For thick alloy coatings, it was established [6, 14] that the increase in current density, leading to the rise in antimony content in the coating, results in the increase in hardness of the deposited layer. This increased hardness can be attributed to the incorporation of antimony in the silver lattice, forming a solid solution (α-phase) and the consequent increase of the silver lattice parameter [6]. After saturation of the silver lattice with antimony leading to increase in the compressive stress in the deposited layers, a new antimony rich phase is deposited, resulting in reduction of the internal stress and of the microhardness of the deposited layers [14].

In multilayer coatings with thicker sublayers, the highest sublayer has a major influence on the microhardness. The Vickers microhardness, Hv, of the deposited coatings was measured in three different positions set at a distance of 2 cm from each other along the sample. Each point of the curves in the respective figures represents the average of at least nine measurements.

Figure 11 shows the Hv values for three different ratios of J. The pulse durations were chosen so that the thickness of the separate sublayers is approximately the same. The IS changes of the multilayer coatings at a current density ratio J_1:$J_2 = 1$ A dm^{-2}: 0.5 A dm^{-2} are presented in Figures 1, 2 and 3. The highest sublayer was always the silver-richer sublayer. In curve (a) it corresponds to a current density of 0.5 A dm^{-2} and shows considerably higher Hv values than the almost

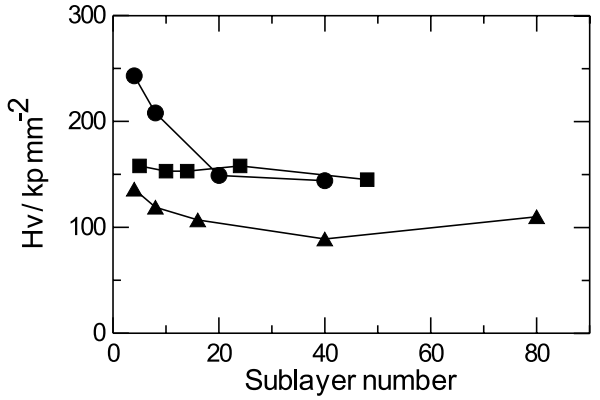

Fig. 11. Microhardness by Vickers of the multilayer coatings depending on the number of sublayers. $C_{Ag} = 16$ g dm^{-3}; $C_{Sb} = 7.5$ g dm^{-3}. Loading 10 p. Ratio of the current densities: (●) J_1:$J_2 = 1$ A dm^{-2}/0.5 A dm^{-2}; t_1:$t_2 = 1$:2; 22 μm (see Figures 1–3). (■) J_1:$J_2 = 1$ A dm^{-2}/0.25 A dm^{-2}; t_1:$t_2 = 1$:4; 26 μm. (▲) J_1:$J_2 = 0.5$ A dm^{-2}/0.25 A dm^{-2}; t_1:$t_2 = 1$:2; 23 μm.

pure silver sublayer deposited at 0.25 A dm^{-2}, which is clearly evidenced by the thick sublayers. The comparison of the two curves (b) and (c) for the low current density (0.25 A dm^{-2}) again reveals the influence of the already deposited layers on the subsequently depositing ones, as already established from the stress measurements. Despite the fluctuations in the experimental values at decreasing antimony content in the multilayer coating due to the contribution of the lower current density, lower values are detected for the microhardness of the multilayer coatings.

The change in microhardness at considerably shorter pulses is shown for another electrolyte in Figure 12. Because of the smaller thickness of the coatings, the measurements are conducted at a load of 2p on the cross section of the samples. When the sublayers are of the same thickness, the increase in their number leads to a decrease in the microhardness (curve (a)). This is probably related to a decrease in the antimony concentration in the coating. Higher microhardness values are registered in the multilayer coatings at pulse parameters leading to another thickness ratio of the separate sublayers and to an increased total antimony content (curve (b)).

3.4. *Wear resistance*

Similarly to the measurements of the thick alloy coatings [14], the wear resistance, A, of the multilayer coatings was determined by the method of Bosch–Weinmann. Figure 13, curve (a) shows the results obtained by the use of an electrolyte of standard composition (16 g dm^{-3} Ag and 7.5 g dm^{-3} Sb). The two curves A–A (0.5 A dm^{-2}) and B–B (1.0 A dm^{-2}) show the respective values for thick alloy layers typical of the current densities applied. Despite fluctuations, the values are averaged between the two limiting cases. Substantial changes in wear resistance depending on the number of sublayers are not observed. It was already shown that the alloys deposited at a higher current density are of lower wear resistance due to the contribution of the antimony-richer phase [14]. Here, the influence of the higher current density is also manifested in the reduced wear resistance of the multilayer coatings compared to those deposited at lower current density. This means that the deposition of multilayer coatings from silver–antimony alloy aimed at increasing the wear resistance of silver would be reasonable only at a very low antimony content in the alloy.

Such a case is realizable at different current densities of the same ratio, for example, 0.5 A dm^{-2}: 0.25 A dm^{-2} (Figure 13, (b)). In this case, high wear resistance is achieved and its values at extremely low sublayer thickness seem to be slightly increased.

The wear resistance also increases with reduction in the high current density contribution and probably with increase in the silver-richer phase in the coating. The results show that higher wear resistance is detected for

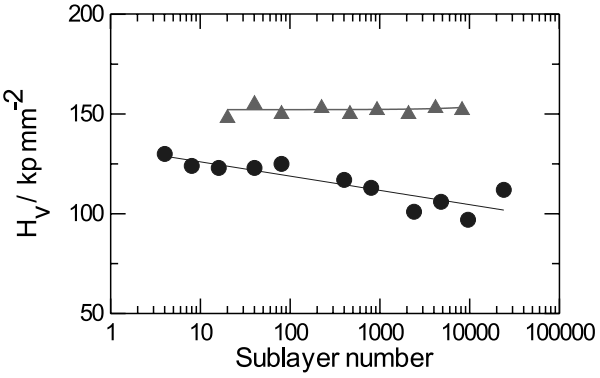

Fig. 12. Microhardness by Vickers of the multilayer coatings depending on the number of sublayers. $C_{Ag} = 16$ g dm^{-3}; $C_{Sb} = 5.0$ g dm^{-3}; KAg $(CN)_2$ electrolyte. Loading 2 p. Measurement in the cross-section of the deposit. Vickers microhardness of the copper substrate $Hv_{0.002} = 112$ kp mm^{-2}. Ratio of current densities: (▲) J_1:$J_2 =$ 0.25 A dm^{-2}/1.0 A dm^{-2}; t_1:$t_2 = 2.2$:1; 17 μm and (●) J_1:$J_2 = 0.5$ A dm^{-2}/0.25 A dm^{-2}; t_1:$t_2 =$ 1:2; 12 μm.

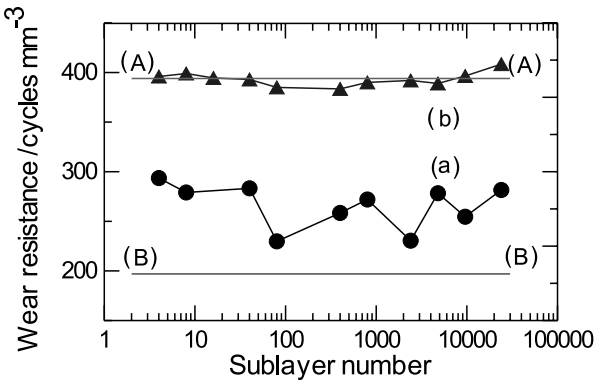

Fig. 13. Wear resistance depending on the number of sublayers. For curve (a): (●) $C_{Ag} = 16$ g dm^{-3}; $C_{Sb} = 7.5$ g dm^{-3}; J_1:$J_2 = 1$ A dm^{-2}/0.5 A dm^{-2}; t_1:$t_2 =$ 1:2: average thickness 22 μm. For curve (b): (▲) $C_{Ag} = 16$ g dm^{-3}; $C_{Sb} = 5.0$ g dm^{-3}; KAg $(CN)_2$ electrolyte; J_1:$J_2 =$ 0.5 A dm^{-2}/0.25 A dm^{-2}; t_1:$t_2 =$ 1:2; average thickness 12 μm. (A–A) 0.5 A dm^{-2}; (B–B) 1.0 A dm^{-2}.

the unstrained layers, while for layers of high compressive stress the wear resistance is considerably lower.

3.5. *Roughness*

The roughness, *Ra*, of the multilayer alloy coatings differs slightly from that of the monolayer alloys deposited in the presence of antimony. By codeposition of antimony, due to the effects of brightening and of grain size reduction, layers of considerably higher smoothness were obtained as compared to the pure silver coatings [14]. No dependence of the roughness of the multilayer alloy coating on the number of sublayers was established. In all cases the *Ra* value of the deposits was less than 1 μm.

3.6. *Plug-in forces*

The measurement of the plug-in forces, F, was carried out on contact pins and jacks using a set up constructed by FEM, similarly to the measurements on the thick alloy coatings [14]. The negative sign of the forces in this study corresponds by definition to the introduction of the pin into the jack. The reduction in the sublayer thickness enhances the plug-in forces. Figure 14 shows the dependence of F on the sublayer number, thus revealing the influence of the increased number of interfaces. A maximum in F is observed at a sublayer thickness of about 0.03 μm and the values decrease again with further reduction of the pulse duration. This is probably due to the worsening of the effect of high current density at the extremely short pulses and to the formation of more homogeneous layers under such conditions.

It can be concluded that at an antimony concentration of 7.5 g dm^{-3} and at very high number of the sublayers, the initially increasing plug-in forces decrease at constant roughness and wear resistance, at reduced microhardness and unchanged contact resistance. The internal stress can be modified arbitrarily by appropriate variation of the deposition conditions.

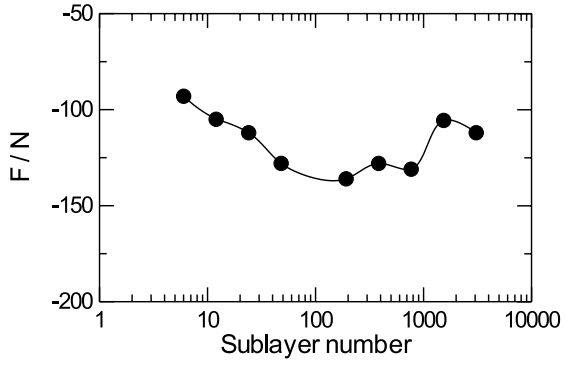

Fig. 14. Plug-in forces depending on the number of sublayers. Total thickness 6 μm. $C_{Ag} = 16$ g dm^{-3}; $C_{Sb} = 7.5$ g dm^{-3}. $J_1{:}J_2 = 1.0$ A dm^{-2}/0.5 A dm^{-3}; $t_1{:}t_2 = 1{:}2$.

4. Conclusions

In electrolytic deposition of multilayer systems based on silver–antimony alloys, coatings of modified properties can be obtained. The internal stress of the first thick sublayers corresponds to the internal stress of the thick alloy layers, and the internal stress of the subsequent sublayers is influenced by the previous ones. The influence of the antimony-richer sublayer increases up to certain limits with reduction in sublayer thickness, whereupon at very short current pulses the effect of the higher current density cannot be realized.

By variation of the pulse parameters, the internal stress of the multilayer systems can be conveniently modified in order to obtain coatings of compressive stress, tensile stress or unstrained coatings. The electrical contact resistance is of approximately constant value regardless of the sublayer thickness. The microhardness of the multilayer systems increases with the increasing contribution of the higher current density, that is, with increasing antimony content in the multilayer coating. At very short pulses a reduction is observed in the microhardness, which is attributable to the deleterious effect of the higher current density.

The values of the wear resistance are between those of the thick alloy coatings deposited at the respective current densities. In some cases at very short pulses the wear resistance increases. It also increases with reduction in the contribution of the high current density. The unstrained coatings are of higher wear resistance.

The roughness of the multilayer coatings corresponds to the roughness of the deposited alloys in the presence of antimony and is not influenced by the sublayer thickness.

The plug-in forces of the multilayer coatings increase with reduction in the sublayer thickness. At very short current pulse durations, they again decrease due to the effect of the higher current density.

Acknowledgements

The present studies are part of a joint research project between the Institute of Physical Chemistry of the Bulgarian Academy of Sciences, Sofia and Forschungsinstitut für Edelmetalle und Metallchemie, Schwäbisch Gmünd. The authors express their gratitude to Deutsche Forschungsgemeinschaft for financial support of project 436 Bul 113/97/0-2.

References

1. A. Brenner, '*Electrodeposition of alloys*', Vol. I, (Academic Press, New York, 1963), p. 609.
2. P.M. Vjacheslavov, S.J. Grilihes, G.K. Burkat and E.G. Kruglova, '*Galvanotechnika blagorodnih i redkih metallov*' (Leningrad, Mashinostroenie 1970), p. 5 (in Russian).
3. P.M. Vjacheslavov, '*Novie elektrokhimicheskie pokritija*' (Leningrad, Lenizdat 1972), p. 213 (in Russian).
4. I. Kristev and M. Nikolova, *J. Appl. Electrochem.* **16** (1986) 875.

5. I. Krastev, A. Zielonka, S. Nakabayashi and K. Inokuma, *J. Appl. Electrochem.* **31**(9) (2001) 1041.
6. I. Krastev and M. Nikolova, *J. Appl. Electrochem.* **16** (1986) 867.
7. I. Krastev, M. Nikolova and I. Nakada, *Electrochim. Acta* **34**(8) (1989) 1219.
8. I. Krastev, *Bulg. Chem. Commun.* **29**(3/4) (1996/97) 586.
9. S. Nakabayashi, K. Inokuma, A. Nakao and I. Krastev, *Chem. Lett.*, Chemical Society of Japan (2000) 88.
10. I. Krastev, M.E. Baumgärtner and Ch.J. Raub, *Metalloberfläche* **46**(2) (1992) 63.
11. I. Krastev, M.E. Baumgärtner and Ch.J. Raub, *Metalloberfläche* **46**(3) (1992) 115.
12. S. Nakabayashi, I. Krastev, R. Aogaki and K. Inokuma, *Chem. Phys. Lett.* **294** (1998) 204.
13. H.R. Khan, O. Loebich, I. Krastev and Ch.J. Raub, *Trans. Inst. Metal. Finish.* (*UK*) **72**(4) (1994) 134.
14. I. Krastev, N. Petkova and A. Zielonka, *J. Appl. Electrochem.* **32**(7) (2002) 811.
15. M. Monev, I. Krastev and A. Zielonka, *J. Physics: Condens. Matter* **11** (1999) 10033.
16. J-P. Celis, K. van Acker, K. Callewaert and P. van Houtte, *J. Electrochem. Soc.* **142** (1995) 70.
17. E. Chassaing, *J. Electrochem. Soc.* **144** (1997) L328.
18. M. Stalzer, *Metalloberfläche* **18** (1964) 263.